34th Annual International Conference of the IEEE EMBS
San Diego, California USA, 28 August - 1 September, 2012

Detection of motion artifacts in photoplethysmographic signals based on time and period domain analysis

R. Couceiro, P. Carvalho, R. P. Paiva, J. Henriques and J. Muehlsteff

Abstract— **The presence of motion artifacts in the photoplethysmographic (PPG) signals is one of the major obstacles in the extraction of reliable cardiovascular parameters in real time and continuous monitoring applications. In the current paper we present an algorithm for motion artifact detection, which is based on the analysis of the variations in the time and period domain characteristics of the PPG signal. The extracted features are ranked using a feature selection algorithm (NMIFS) and the best features are used in a Support Vector Machine classification model to distinguish between clean and corrupted sections of the PPG signal. The results achieved by the current algorithm (SE: 0.827 and SP: 0.927) show that both time and especially period domain features play an important role in the discrimination of motion artifacts from clean PPG pulses.**

I. Introduction

Photoplethysmography (PPG) is a non-invasive, low cost tool to continuously monitor blood volume changes in tissue as a function of time. It has been accepted by the International Standards Organization (ISO) and the European Committee for Standardization as the standard non-invasive measure of oxygen saturation level since 1987 [1]. Moreover, this technique has been widely applied in many clinical areas such as anesthesia, surgical recovery and critical care.

Motivated by unmet needs in low cost, non-intrusive and portable techniques in p-Health, the PPG technique has been object of an extensive research in the later decades. Due to technological advances in the field of opto-electronics, clinical instrumentation and digital signal processing, the PPG technique achieved a broader spectrum of potential applications, ranging from the field of clinical physiological monitoring to the vascular assessment, and autonomic function evaluation [2].

However, PPG signals can be easily influenced in the measurement process which may lead to inaccurate interpretation of the PPG waveform. Well-known sources of error are ambient light at the photodetector, poor blood perfusion of the peripheral tissues and motion artifacts [3]. In uncontrolled environments such as the primary and home care settings, these potential error sources are more frequent and can become a serious obstacle to the reliable use of PPG derived parameters in real time and continuous monitoring applications. Therefore, it is essential to provide a signal quality or trust metric that provides the subsequent analysis algorithms with a level of trust in the derived parameters.

Although the recent technological advances allowed the minimization of some of these limitations, motion artifact detection and suppression is still a major challenge in research. Indeed, the field of motion artifact and noise suppression has been subject of intensive research in the last decade. Various approaches have been investigated, where the corrupted signal is recovered or reconstructed by applying signal processing techniques such as adaptive filtering techniques [4-6], time-frequency analysis [7, 8] and source separation techniques [9]. However, PPG signals severely contaminated by noise and motion artifacts show dramatic changes in the waveform morphology, which compromise the signal quality and therefore its suitability for further analysis. An alternative is the robust detection of PPG signal sections corrupted by noise and motion artifacts. Techniques such as morphological analysis [3] and higher-order statistical analysis [10] have been proposed in this research field.

In this paper, a motion artifact detection algorithm is presented. The proposed methodology is based on the analysis of the time and period domain characteristics of the PPG signal. The NMIFS algorithm [11] is used to select the most relevant features which are used as inputs to a Support Vector Machine (SVM) classification model.

The reminder of the current paper is organized as follows. In section II, the experimental protocol is presented. The proposed methodology is introduced in section III. The results and respective discussion are presented in section IV. Finally, the conclusions are summarized in section V.

II. Experimental protocol

To evaluate the performance of the proposed algorithm, a data collection study was conducted in the Faculty of Sciences and Technology of the University of Coimbra aiming at the simultaneous collection of electrocardiographic (ECG) and photoplethysmograpic (PPG) signals from 8 healthy volunteers, aged 27.3 ± 3.7 years and with BMI 24.4 ± 2.8 kg/m^2.

The PPG waveform was recorded from the tip of the index finger using the transmissive mode infrared finger probe, while the ECG was recorded using Einthoven-II lead configuration. The PPG and ECG signals were recorded using a HP-CMS monitor and were digitized at a sampling frequency of 125 Hz and 500 Hz, respectively.

In order to conduct a wide variety of motion artifact patterns, the subjects were asked to execute two runs of eleven different types of hand and body movements,

This work was supported in part by the EU FP7 project HeartCycle (FP7 – 216695).

R. Couceiro, P. Carvalho, R. P. Paiva and J. Henriques are with the University of Coimbra, Department of Informatics Engineering, Science and Technology Faculty of the University of Coimbra, Pólo II, Coimbra, Portugal (e-mail: {rcouceir, carvalho, ruipedro, jh}@dei.uc.pt).

J. Muehlsteff is with Philips Research Laboratories Europe, Eindhoven, Netherlands, (e-mail: {Jens.Muehlsteff}@philips.com).

resulting in 22 records of 60 seconds for each subject. The movements are described as follows: 1) Disturbance of the PPG probe, causing variations in the contact point between fingertip and probe; 2) Gently bending of the index finger; 3) Repeated movement of the wrist left and right; 4) Shaking the wrist; 5) Repeated movement of the epsilateral arm in the horizontal plane; 6) Repeated movement of the epsilateral arm in the vertical plane; 7) Lifting and lowering a book with both hands; 8) Repeated tapping of the table with the index finger; 9) Repeated raising and lowering of the arm; 10) Repeated sitting down and standing up; 11) Slow walking in a straight line. Each of the movements was performed in the 20 seconds centre epoch of the record. The records were annotated by a clinical expert.

III. METHODS

The proposed methodology for the detection of motion artifacts consist in the following stages: a) Pre-processing and baseline removal; b) Segmentation; c) Feature extraction; d) Feature selection and e) Classification.

A. Pre-processing

The goal of the pre-processing stage is to remove the frequency components that do not represent the fundamental features of the PPG signal. Firstly, the spectral components above 18Hz are filtered using a 7th order low-pass Butterworth filter. Additionally, a 2 second window moving average filter is applied to derive an approximation of the PPG signal baseline with spectral content below 0.23Hz, which is subtracted from the original PPG signal.

B. Segmentation

In the segmentation step, the PPG signal is firstly differentiated using a five-point digital differentiator, resulting in 1st to 3rd order derivatives. To detect the PPG pulses, a histogram based threshold detection algorithm was applied to detect the most significant local maxima of the 1st derivative and the corresponding local minima of the 3rd derivative. The PPG beat onset/offset was defined to be the most relevant peak prior to the detected most relevant valley.

C. Feature extraction

The feature extraction approach is based on the analysis of the time and period domain characteristics of the PPG signal. In the time domain analysis, the main morphological characteristics of the PPG pulses are assessed resulting in 7 features. In the period domain analysis, the characteristics of principal components of the period spectrum and their relationships are evaluated, leading to the extraction of 19 features. In summary, 26 features were extracted from the time and period domain analysis.

1) Time domain analysis

The morphology of the PPG pulses and their relationships with the neighboring pulses are analyzed, leading to the definition of the following characteristics: 1) pulse amplitude; 2) pulse length; 3) pulse rate; 4) trough depth difference; 5) peak height difference; 6) pulse skewness; and 7) pulse kurtosis.

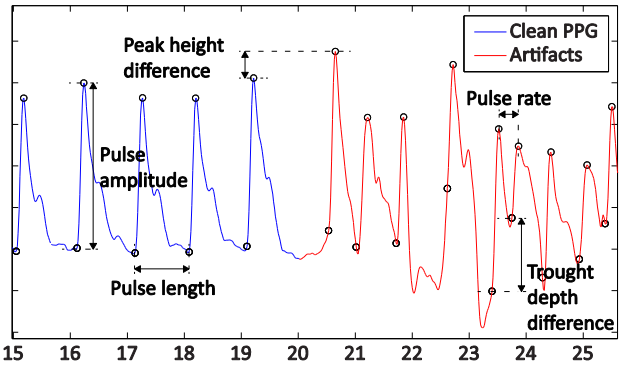

Figure 1. Time domain characteristics of the PPG data.

As illustrated in Figure 1 the pulse amplitude is defined as the difference between the pulse peak height and its preceding trough depth (pulse onset), the pulse length is the time interval between the onset of two consecutive pulses and the pulse rate is the time interval between maxima of two consecutive pulses. The difference between the peak height and peak depth of two consecutive pulses was also considered. Furthermore, the symmetry and "peakedness" of the PPG pulses are assessed using skewness and kurtosis measures, respectively. From the analysis of various types of PPG pulses, we observed that when motion artifacts are present, the aforementioned characteristics vary significantly. Contrarily, in clean PPG signals the PPG pulses are similar and therefore there is almost no variation in its characteristics. To capture these variations, the change in the pulse characteristics is evaluated using eq. (1), resulting in the features F_1 to F_7.

$$F_i = f_{\varnothing}(C_i) = |C_i(j) - C_i(j-1)| \quad (1)$$

where, c_i is the i^{th} characteristic and j is the pulse (section) index.

2) Period domain analysis

To assess the periodic characteristics of the PPG signal, the Discrete-time Short Time Fourier Transform (STFT) was applied. Let the $[x_n, \ldots, x_{n+L-1}]$ be the sequence defining the section of the PPG signal under analysis. For a sampling frequency F_s, the frequency "bin" k of the N-point STFT corresponds to the frequency $f_k = k.F_s/N$ Hz, and

$$X(n,k) = \sum_{m=0}^{L-1} x[n+m]w[m]e^{-j(2\pi/N)km} \quad (2)$$

is the expression for the DFT of the windowed sequence $x[n+m]w[m]$ of the k[th] frequency bin. To derive the STFT in the period domain, let $s=1,2,\ldots,N-1$ samples be the range of possible periods in the aforementioned sequence. The frequency f_k corresponds to the period $s_k = 1/f_k = N/(k.f_s)$ seconds $= N/k$ samples. Substituting into (2), for the period s, gives the STFT in the period domain, i.e. PD-STFT.

$$X(n,s) = \sum_{m=0}^{L-1} x[n+m]w[m]e^{-j2\pi m/s} \quad (3)$$

To choose the size of the sequences (L) and the forward step (Δn), that is related to the section overlapping (L-Δn) one must take into account: i) the stationarity of the analyzed signal section; ii) the tradeoff between the PD-STFT period

and temporal resolution; iii) the temporal resolution needed for the subsequent analysis.

Considering the aforementioned issues, the PD-STFT was applied using a rectangular-shaped sliding window with approximately 3 times the fundamental period of the PPG signal and the overlap between consecutive windows was set to be approximately 85%. Thus, we assume the stationarity of the signal in the analyzed section and guarantee an appropriate frequency resolution of the computed PD-STFT. Furthermore, by choosing 85% window overlap size we ensure that the analysis output has the temporal resolution necessary for further analysis and motion artifact detection. The fundamental period was extracted and updated based on the periodic analysis of small sections (5s) of the PPG signal.

The resulting stream of period domain spectra goes into analysis for feature extraction. The feature extraction procedure resorts on the principle that, similarly to the morphology of the PPG signal, the PD-STFT also exhibits a regular shape representing the main features of the signal. From an analysis of the PD-STFT of various classes of PPG [12] one observed that the PD-STFT of a clean PPG signal consists of three major spikes with different locations, lengths and amplitudes. The most relevant spike corresponds to the fundamental period of the PPG signal, i.e. the length of the cardiac cycle (beat). The remaining spikes are thought to be associated with the location and amplitude of the waves reflected from the periphery towards the aorta. Based on these assumptions, the power spectra of several uncorrupted and motion corrupted PPG sections were analyzed. We observed that the power spectra of PPG sections corrupted with motion artifacts presented several random components that do not represent the fundamental characteristics of the underlying uncorrupted signal, resulting in a random and significant change in the period domain characteristics.

To capture these variations, the PD-STFT of each PPG section was analyzed and the following characteristics were defined (see Figure 2)): 1) height (H); 2) location (L); 3) width (W); and 4) area (A). These characteristics were evaluated for each of the three most relevant spikes (C_i^{Pj},*for i=1,…,4 and j=1,2,3*). Additionally, the relationship between characteristics of the two most relevant peaks (P_1 and P_2) was also assessed and defined as follows:

$$M_i = C_i^{P1} - C_i^{P2}, \quad i = 1, \dots, 4 \tag{4}$$

The area of the remaining spectrum (C_4^{RS}) and its relationship with the area of the three most relevant peaks was also considered:

$$M_5 = \frac{C_4^{RS}}{C_4^{P1} + C_4^{P2} + C_4^{P3}} \tag{5}$$

From abovementioned analysis 18 features (F_8 to F_{25}) were extracted, corresponding to the rate of change (see eq. (1)) of the aforementioned characteristics.

Assuming that the main periodic characteristics of the PPG signal are represented by the most relevant components in the distribution and that the remaining components are the result of noise and motion artifacts, a model of the original

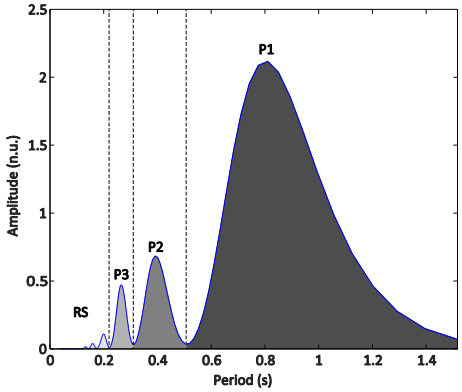

Figure 2. Major components of the PPG signal in the period domain.

distribution was created based on the 3 most relevant spikes, using Gaussian functions. The parameters of each Gaussian are determined based on the height, location and width of the detected spikes. The comparison between the computed model (X_m) and the original distribution (X_o) is then evaluated using Kullback–Leibler divergence measure (eq. (6)).

$$F_{26} = D_{KL}(X_m; X_o) = \sum_i X_m(i) \ln\left(\frac{X_m(i)}{X_o(i)}\right) \tag{6}$$

The rationale behind this comparison is that the increase in the spectrum complexity, as a result of the inclusion of random components, can be detected by an increase in the Kullback–Leibler divergence.

D. *Feature selection*

In the features selection step, the objective is to select a subset that contains the most relevant and least redundant features for the discrimination of motion artifacts, enabling an enhanced performance of the classification model to be built upstream. Additionally, improvements can be expected in classification model's generalization capability and interpretability. The feature selection was performed using the algorithm NMIFS [11] which is based on the maximization of the normalized mutual (nMI) information between the extracted features and the classes, and minimization of the inter-feature nMI. Additionally, a ROC analysis was also performed to evaluate the capability of each feature to discriminate motion artifacts from clean PPG.

In Figure 3 we present the scores of the extracted features, that is: i) the NMIFS "score"; ii) the feature

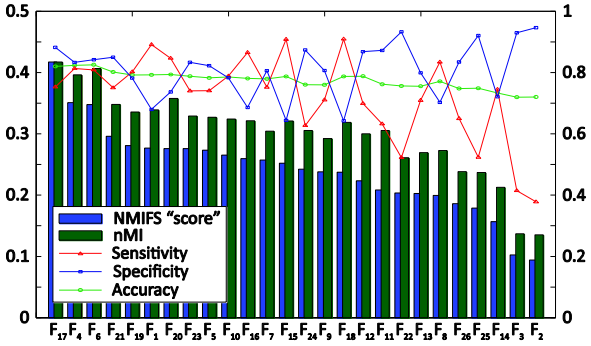

Figure 3. NMIFS and ROC analysis "scores" for the 26 extracted features.

relevance (nMI); and iii) the ROC analysis scores (sensitivity, specificity and accuracy for the optimal threshold). From the analysis of the computed scores, the 8 most relevant features were selected, corresponding to 3 features from the time domain (F_1,F_4 and F_6) and 5 features from the period domain (F_{17}, $F_{19,\ldots,21}$, F_{23}).

E. Classification

A Support Vector Machine (SVM) has been adopted for the discrimination between motion artifacts and clean PPG. The classification process was performed using the algorithm C-SVC [13], with a radial basis function kernel.

In order to find the parameters gamma (γ) and cost (C) that better suit the present classification problem, a grid-search method using 10-fold cross-validation was used.

The proposed methodology was validated using a 10-fold cross-validation scheme and repeated 20 times.

IV. Results and Discussion

The 176 recorded signals were analyzed and each section was classified using the proposed methodology and compared to the manually annotated classification. The performance of the algorithm was evaluated using a 10-fold cross validation scheme with the following metrics: sensitivity (SE) and specificity (SP), and accuracy (ACC).

As can be observed in TABLE I the algorithm achieved a good performance in the classification of both corrupted and clean PPG sections, with an overall accuracy of 88.6%. From TABLE I it can be observed that the majority of the movement artifacts are identified with an accuracy over 0.9. On the other hand, there is decrease in the detection performance for 4 movement artifacts, which is possibly associated with low corruption of the PPG data and/or an increase in the periodicity in the performed movements.

V. Conclusion

In the current paper a novel algorithm for the detection of motion artifacts in photoplethysmographic signals has been proposed. The discrimination between motion artifact corrupted and uncorrupted pulses was performed based on the analysis of the PPG signal only in the time and period domain, resulting in the extraction of 26 features. In order to simplify the classification model, the extracted features were ranked using the NMIFS algorithm with 8 selected features. The discrimination between corrupted and clean pulses was performed using an SVM model.

The proposed model was tested in 8 subjects, and 11 different motion sources. To validate the proposed algorithm a 10-fold cross-validation scheme was repeated 20 times. The results achieved by the current algorithm (SE: 0.827 and SP: 0.927) suggest that the characteristics of periodic components of the PPG signal can be used as discriminative features for motion artifact detection.

Future work will focus on the extraction of more discriminative features. According to [10], the clean and corrupted PPG data exhibit different bispectral characteristics which can be used to improve the performance of the current algorithm.

TABLE I. Performance results of the proposed algorithm

Context	*Performance metric (avg ± std)*		
	SE	***SP***	***ACC***
All movements	0.827±0.01	0.927±0.007	0.886±0.006
Movement 1	0.865±0.041	0.932±0.021	0.905±0.017
Movement 2	0.893±0.037	0.953±0.016	0.930±0.020
Movement 3	0.561±0.043	0.958±0.017	0.794±0.025
Movement 4	0.816±0.038	0.955±0.015	0.902±0.019
Movement 5	0.753±0.044	0.910±0.024	0.847±0.028
Movement 6	0.881±0.028	0.943±0.021	0.920±0.017
Movement 7	0.883±0.021	0.947±0.014	0.919±0.017
Movement 8	0.721±0.046	0.913±0.030	0.835±0.019
Movement 9	0.843±0.027	0.904±0.028	0.876±0.018
Movement 10	0.923±0.018	0.886±0.033	0.903±0.018
Movement 11	0.938±0.024	0.898±0.030	0.915±0.020

References

[1] A. B. Shang, *et al.*, "Development of a Standardized Method for Motion Testing in Pulse Oximeters," *Anesthesia & Analgesia,* vol. 105, pp. S66-S77, December 2007 2007.

[2] J. Allen, "Photoplethysmography and its application in clinical physiological measurement," *Physiological Measurement,* vol. 28, p. R1, 2007.

[3] J. A. Sukor, *et al.*, "Signal quality measures for pulse oximetry through waveform morphology analysis," *Physiological Measurement,* vol. 32, p. 369, 2011.

[4] J. Foo and S. Wilson, "A computational system to optimise noise rejection in photoplethysmography signals during motion or poor perfusion states," *Medical and Biological Engineering and Computing,* vol. 44, pp. 140-145, 2006.

[5] J. M. Graybeal and M. T. Petterson, "Adaptive filtering and alternative calculations revolutionizes pulse oximetry sensitivity and specificity during motion and low perfusion," in *Engineering in Medicine and Biology Society, 2004. IEMBS '04. 26th Annual International Conference of the IEEE*, 2004, pp. 5363-5366.

[6] S. Kunchon, *et al.*, "Comparative evaluation of adaptive filters in motion artifact cancellation for pulse oximetry," in *Signal Processing & Its Applications, 2009. CSPA 2009. 5th International Colloquium on*, 2009, pp. 307-311.

[7] K. A. Reddy, *et al.*, "Motion Artifact Reduction and Data Compression of Photoplethysmo-graphic Signals utilizing Cycle by Cycle Fourier Series Analysis," in *Instrumentation and Measurement Technology Conference Proceedings, 2008. IMTC 2008. IEEE*, 2008, pp. 176-179.

[8] Y.-s. Yan, *et al.*, "Reduction of motion artifact in pulse oximetry by smoothed pseudo Wigner-Ville distribution," *Journal of NeuroEngineering and Rehabilitation,* vol. 2, p. 3, 2005.

[9] B. S. Kim and S. K. Yoo, "Motion artifact reduction in photoplethysmography using independent component analysis," *Biomedical Engineering, IEEE Transactions on,* vol. 53, pp. 566-568, 2006.

[10] R. Krishnan, *et al.*, "Analysis and detection of motion artifact in photoplethysmographic data using higher order statistics," in *Acoustics, Speech and Signal Processing, 2008. ICASSP 2008. IEEE International Conference on*, 2008, pp. 613-616.

[11] P. A. Estevez, *et al.*, "Normalized Mutual Information Feature Selection," *Neural Networks, IEEE Transactions on,* vol. 20, pp. 189-201, 2009.

[12] T. R. Dawber, *et al.*, "Characteristics of the Dicrotic Notch of the Arterial Pulse Wave in Coronary Heart Disease," *Angiology,* vol. 24, pp. 244-255, April 1, 1973 1973.

[13] C.-C. Chang and C.-J. Lin, "LIBSVM : a library for support vector machines. ACM Transactions on Intelligent Systems and Technology," vol. 2, pp. 27:1--27:27, 2011.